An Alternative Body Temperature Measurement Solution: Combination of a Highly Accurate Monitoring System and a Visualized Public Health Cloud Platform

Joe-Air Jiang, *Senior Member, IEEE*, Jen-Cheng Wang, Chao-Liang Hsieh, Kai-Sheng Tseng, Zheng-Wei Ye, Lin-Kuei Su, Chih-Hong Sun, Tzai-Hung Wen, and Jehn-Yih Juang

***Abstract*—To quickly isolate suspected cases to control the epidemics, this study proposes a body temperature monitoring system with a thermography based on the Internet of Things (IoT) architecture. The collected data are transmitted to a back-end platform via wireless communication. Using the analyzed data, the platform provides services, such as instant alerts for any anomalies, infectious disease outbreak prediction, and risk level assessment for a given area, and it will be a great help to epidemic prevention. The mean absolute percentage error and root mean square error of the proposed monitoring system under an extensive series of experiments are 0.04% and 0.0204 °C, respectively. It shows that the body temperature measured by the thermal imaging sensor in the system can accurately represent the actual body temperature after specific calibrations that take the environmental temperature into account. It can also be expanded to a decision supporting system to help schools or government agencies to make proper decisions to stop the spread of infectious diseases.**

***Index Terms*—Body temperature monitoring system, Internet of Things (IoT), risk level, thermal imaging sensor.**

Manuscript received June 21, 2020; accepted October 16, 2020. Date of publication October 27, 2020; date of current version March 24, 2021. This work was supported in part by the Ministry of Science and Technology, and in part by the Council of Agriculture of the Executive Yuan, Taiwan, under the Grant MOST 105-2221-E-002-132-MY3, Grant MOST 106-3113-E-002-012, Grant MOST 107-3113-E-002-007, Grant MOST 108-2321-B-002- 037, Grant MOST 108-2811-B-002-510, Grant MOST 108-2622-E-002-023-CC2, Grant MOST 108-2221-E-002-090, Grant MOST 109-2321-B-002-043, Grant MOST 109-2811-B-002- 521, Grant 108AS-13.2.11-ST-a5, Grant 108AS-16.2.1-FD-Z2, Grant 109AS-11.3.2-ST-a2, Grant 109 AS-14.2.1-FD-Z2, and Grant 109AS-11.3.2-ST-a8. *(Corresponding author: Joe-Air Jiang.)*

Joe-Air Jiang is with the Department of Biomechatronics Engineering, National Taiwan University, Taipei 10617, Taiwan, and also with the Department of Medical Research, China Medical University Hospital, China Medical University, Taichung 40447, Taiwan (e-mail: jajiang@ntu.edu.tw).

Jen-Cheng Wang, Chao-Liang Hsieh, Kai-Sheng Tseng, Zheng-Wei Ye, and Lin-Kuei Su are with the Department of Biomechatronics Engineering, National Taiwan University, Taipei 10617, Taiwan (e-mail: f98631002@ntu.edu.tw; r05631025@ntu.edu.tw; r04631026@ntu.edu.tw; ga683913@gmail.com; h87887887@gmail.com).

Chih-Hong Sun, Tzai-Hung Wen, and Jehn-Yih Juang are with the Department of Geography, National Taiwan University, Taipei 10617, Taiwan (e-mail: chsun@ntu.edu.tw; wenthung@ntu.edu.tw; jjuang@ntu.edu.tw).

Digital Object Identifier 10.1109/JIOT.2020.3034024

I. Introduction

IN RECENT years, people have been paying more and more attention to health care, but the focus is gradually shifting from diagnosis and treatment to prevention [1], especially when deadly diseases are spreading. Some diseases that cause significant damage to human organs have been identified. For example, in 2009, the H1N1 outbreak occurred in 209 countries, with a total death toll as high as 14 142 worldwide [2]. Dengue fever (DF) cases have been often found in tropical and subtropical areas. In Taiwan, up to 15 732 cases were reported in 2014 (Ministry of Health and Welfare Department of Disease Control of Taiwan, 2015) [3]. The middle east respiratory syndrome (MERS), identified recently, is a severe lung infection posing a global threat to human health. In 2012, MERS was found in Middle East and spread fast to the world. A total of 27 countries reported cases of MERS-CoV. Since the September of 2012, WHO has notified of 2,040 laboratory- confirmed cases of infection with MERS-CoV and at least 712 deaths were related to MERS-CoV [3]. These diseases along with other highly infectious diseases have brought great impacts on public health, so that the prevention of infectious diseases becomes an urgent issue. With large-scale outbreaks of infectious diseases, the issue of public health has become the center of attention. The situations are getting worst if the treatment is delayed, which might threaten hundreds of thousands of people.

However, traditional ways of detecting infectious diseases is time consuming and labor intensive. It takes time for infected people to seek medical care, and the diseases are widely spread when they contact other people. Quickly isolating suspected cases is a key to control epidemics of deadly diseases, and high fever is one of the most important symptoms that can be used to determine whether someone is infected. Many patients with infectious diseases show a symptom of high fever during the infection, such as Influenza A viruses and dengue [4], [5]. Thus, by monitoring body temperature and then isolating possibly infected cases, the spread of infectious diseases could be effectively controlled. Measuring body temperature has the following advantages. First of all, measured body temperature

cannot be forged. It often reflects the actual condition of human body. Second, body temperature meters are easy to acquire, so it is convenient for people to use the meters. Third, it is easy to use body temperature to determine whether a person has a fever. In practice, a person is not considered to have a significant fever until the temperature reaches between 37.5 °C and 38.3 °C (99.5 °F and 100.9 °F) [6], [7]. More importantly, body temperature is usually associated with disease severity [8]; the higher the temperature, the severer the disease.

Measuring body temperature is the first step toward infectious disease prevention. To prevent the spread of infectious disease, it is necessary to develop a body temperature monitoring system capable of automatically measuring body temperature, collecting body temperature data, analyzing the data, and providing alerts to the public. The technology of Internet of Things (IoT) can be a great help in constructing such a monitoring system. IoT represents a common concept that network devices have ability to measure different parameters and collect sensed data, and then share the data through the Internet. IoT can connect a variety of things or objects, such as radio frequency identification (RFID) tags, sensors, actuators, and mobile phones. Through unique schemes, these things and objects are able to interact with each other and cooperate with their neighbors to reach common goals [9]. With the IoT technologies, the sensed data can be sent to a cloud and analyzed by a computing platform. Recently, more and more researchers have utilized the IoT technologies in their research papers, especially in healthcare studies.

Thus, an IoT-based body temperature monitoring system is proposed in this study. In the proposed system, the front-end sensing data collected by sensors are sent to a cloud in real time through the Internet, so system users can have a complete picture in terms of the health conditions of people in a public area, and they can take proper action based on the information provided by the cloud service.

II. Related Works

Compared to traditional measurement of body temperature (utilizing tools, such as an ear thermometer, an axillary thermometer, a rectal thermometer and an oral temperature meter), a thermal imaging device measures the body temperature with merits of noncontacting, time and labor saving, and easy operation [10]. During the outbreaks of SARS, for example, many international airports used image temperature monitoring systems to find out if the passengers with a high fever when they passed through the immigration [11], [12]. Such a method can effectively identify passengers who need to seek medical attention. However, this method requires manpower to observe temperature changes through the thermal imaging device all the time, resulting in difficulties in widespread use and information management.

IoT applications have been widely used in real-time monitoring, patient information management, and healthcare management and brought convenience to physicians and patients [13]–[29]. For example, a body sensor network (BSN) is one of the core IoT technologies applied to healthcare systems. In BSNs, a patient can be monitored by a collection of tiny-powered and lightweight wireless sensor nodes [13]. With IoT technologies, some health care services and applications have also been proposed [14]–[17]. Moreover, a very diversified applications based on the IoT architecture have also been done in the past, such as children health information [18]–[20], adverse drug reaction [21]–[24], blood pressure monitoring [25], [26], and medication management [27]–[29]. Combined with emerging technologies, such as special sensing devices, 5G, artificial intelligence, and machine learning, IoT architecture will have the potential to play an important role in the research area of public health-related issues, especially the early detection and warning platform for various epidemic diseases with fever symptoms.

Based on the IoT technology, an alternative body temperature measurement and monitoring system is proposed in this study. The proposed system mainly consists of a highly accurate monitoring system and a visualized public health cloud (PHC) platform. The system uses the thermal imaging device to measure the body temperature and further estimate the actual body temperature after specific calibrations that take the environmental temperature into account. Then, the body temperature measurements collected by monitoring system are further sent to a PHC platform. Based on the cloud service and the response guideline for epidemic diseases, the proposed system can provide the instant alerts and classifications of risk levels, and help management or medical personnel to control infectious disease spreading.

III. Material and Methods

A. System Architecture

The proposed system uses thermography inspection as a monitoring method. The framework of the proposed body temperature monitoring system is shown in Fig. 1. The architecture of the proposed system includes a front-end body temperature monitoring system and a back-end control platform. The front-end monitoring system consists of two subsystems: 1) a body temperature detection system and 2) an ambient temperature/humidity sensing system. The body temperature detection system combines a thermal imaging camera developed by CHINO and an embedded platform (i.e., BeagleBoard-xM, Digi-Key Electronics). And the ambient temperature/relative humidity sensing system is composed of an Arduino Uno and a temperature/relative humidity sensor. On the other hand, the back-end platform comprises of a database, a server, and some specially designed algorithms to serve as a PHC, which can analyze the data of the thermograms of each targeted region and environmental temperature/relative humidity. The PHC is also able to provide a variety of services, such as sending out an instant alert for any anomalies, infectious disease spreading prediction, and risk level classification. The system has been installed in two buildings in the campus of National Taiwan University (NTU) to conduct a series of experiments to validate the system performance. The two buildings, one is at the Department of Geography and the other one is at the Department of Biomechatronics Engineering, are separated around 700 m.

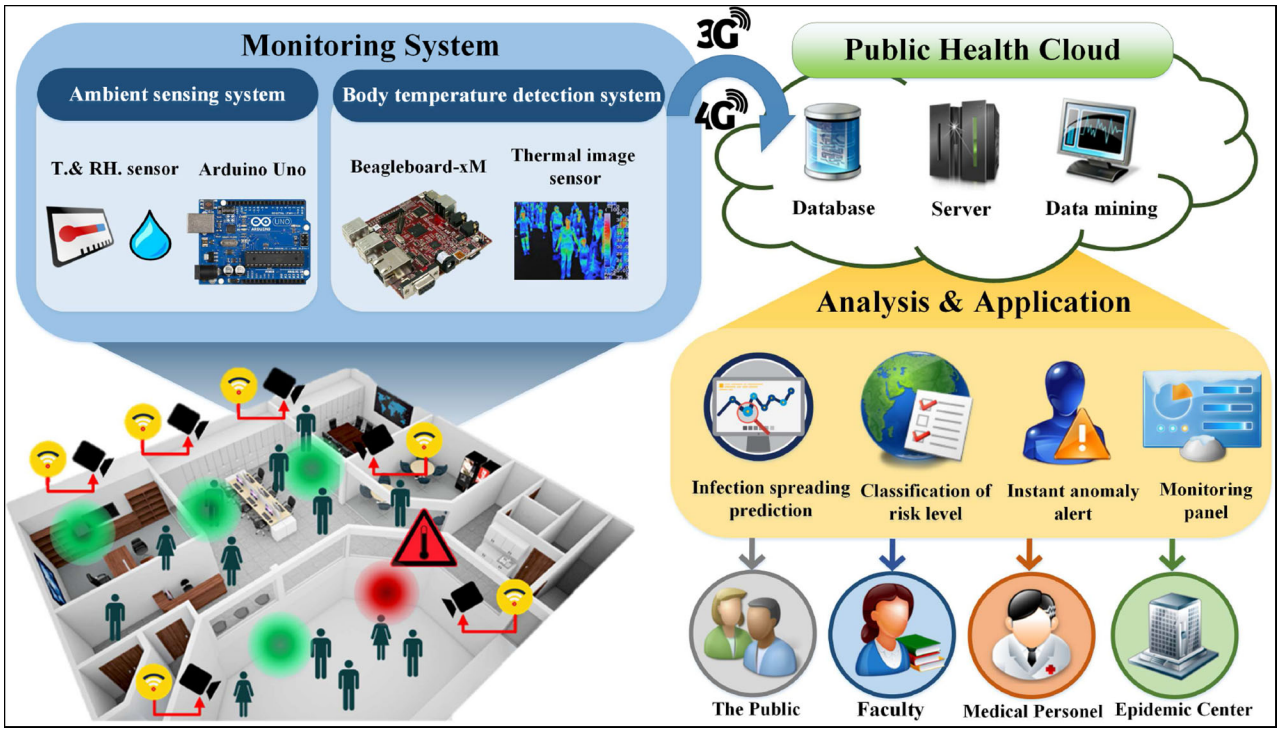

Fig. 1. Framework of the proposed body temperature monitoring system.

The proposed system can monitor the body temperatures of people, who are entering in and out a campus building, to determine if the building is a risk area caused by high-infectious people. The monitoring data are transmitted to a back-end platform through wireless communication for further spatial-temporal diffusion pattern analysis. The analyzed results are sent to administration personnel via an interface on a mobile phone. The proposed system also automatically sends out instant alert messages. These alert messages provide important disease outbreak information. With the proposed system, epidemic control at the campus can be greatly improved.

B. Front-End Body Temperature Monitoring System

The hardware components of the body temperature detection system and the ambient temperature/humidity sensing system in the proposed monitoring system and their functions are described as below

1) Body Temperature Detection System: The body temperature detection system has three major parts: 1) wireless sensor nodes; 2) a body temperature detection sensor; and 3) a communication module. The functions of each part are introduced as follows.

1) *Wireless Sensor Nodes:* A BeagleBoard-xM (Beagleboard by PTI) serves as the wireless sensor node in this study. The BeagleBoard-xM wirelessly transmits sensed data to the back-end platform via a communication module. It mainly consists of an OMAP DM3730 processor (Texas Instruments Inc.), a low-power DDR RAM of 512 MB, a four-port high-speed Universal Serial Bus (USB) 2.0 hub, a 10/100 Ethernet, and an extended sensor board connecting to external sensors. An external CR2016 lithium-manganese coin battery is used to activate the real-time module on the BeagleBoard-xM. The time on the BeagleBoard-xM is synchronized with the Central Standard Time to ensure that the BeagleBoard-xM can operate at a given time and perform tasks for the back-end platform. The monitoring data are tagged with a time stamp to collect the information regarding the operation hours of the BeagleBoard-xM in an outdoor environment. It is noted that the connections of the sensor board can be extended to various external sensors, but in this study only the temperature, relative humidity, and thermal imaging sensors are used and connected to the sensor board. Table I shows the specifications of the BeagleBoard-xM and other commonly used embedded development boards.

TABLE I
SPECIFICATIONS OF THE BEAGLEBOARD-XM AND TWO COMMONLY USED EMBEDDED DEVELOPMENT BOARDS: KS_2410 & MINI 6410

Device	Processor	Memory (MB)	PCB (cm^2)	Cost (USD)
BeagleBoard-xM	1 GHz	512	7.62 × 7.62	45 to 149
KS_2410	200 MHz	64	13.00 × 10.00	150
Mini 6410	533 MHz	256	11.00 × 11.00	140

2) *Body Temperature Sensor:* Thermal imaging technology plays an important role in the proposed body temperature monitoring system. A thermal image sensor can easily capture the body temperature of a person in a building or an indoor environment. The thermal image sensor used in this study, TP-H2060AN, is developed by a Japanese company, CHINO [30]. The thermal image sensor is a small infrared sensor capable of using an

infrared lens to capture temperature images and sends out an alert with blue lights in real time. It provides an Ethernet port to connect to a PC via the software developed by CHINO to read the thermograms. The length, width, and height of the thermal image sensor are 62, 59, and 72 mm, respectively. It has the advantage of a small size and easy installation. The power of the thermal image sensor is supplied by 110 V. It detects a temperature ranging from—20 °C to 300 °C.

3) *Communication Module:* In this study, a 3G module connects to the BeagleBoard-xM through a USB 2.0 hub, and an MDM 8220 chip is used by the module. The 3G Dongle Modem (E372u USB, Huawei) is used to transmit sensed data to the back-end database. Its speed is 42 and 5.76 Mb/s for uplink and downlink, respectively. Different modes, each with an individual operating frequency, can be selected during the operations. Its advantages are easy connection, high speed downlink/uplink, and operated under different modes.

2) Ambient Temperature and Relative Humidity Sensing System: In this study, SHT11 (Sensirion AG, Switzerland), a surface mountable relative humidity and temperature sensor, is used as the temperature/relative humidity sensor. The SHT11 integrates sensor elements with signal processing components on a tiny foot print and provides a fully calibrated digital output. A unique capacitive sensor element is used for measuring relative humidity, while temperature is measured by a band-gap sensor. With the capacitive sensor and the band-gap sensor, relative humidity and temperature can be measured at the same time.

The SHT11 is seamlessly coupled to a 14-bit analog to digital converter and a serial interface circuit. This results in superior signal quality, a fast response time and insensitivity to external disturbances. The two-wire serial interface and internal voltage regulation allow for easy and fast system integration. The tiny size and low power consumption are the reasons that SHT11 is selected as the temperature and relative humidity sensor. The sensing range of SHT11 for temperature and relative humidity is from −40 °C to 123.8 °C and from 0 to 100% RH, respectively, and the measurement resolution for the two variables is 0.01 °C and 0.05% RH at 25 °C. In addition, the measurement accuracy for the variables is 0.4 °C and 3.0% RH. The sensitivity verification will be presented in the later section.

Moreover, An Arduino Uno (Arduino cc, Italy) is used as a microcontroller board in the sensing system, which is based on the ATmega328P (Atmel). It has 14 digital input/output pins, 6 analog inputs, a USB connection, a power jack, an in-circuit serial programming (ICSP) header, and a reset button. Most important of all, it supports two-wire interface (TWI) communication using the wire library. It connects to the ambient temperature/relative humidity sensor through the TWI. It also establishes a connection with the body temperature detection system.

C. Operation Scheme of the Front-End Body Temperature Monitoring System

The operation procedure of the front-end body temperature monitoring system is shown in Fig. 2. The procedure is divided into three parts. First, BeagleBoard-xM activates the development board and detects whether the system connects to the Internet or not. If the system losses its connection to the Internet, an LED flashes to inform the disconnection to the management personnel. And, the system can be reconnected to the Internet via the 3G module by the management personnel.

Second, with successful Internet connection, BeagleBoard-xM obtains the information of current time and converts the information to the one with the string format. Then it gains access to the port of the thermal image sensor. When a person passes through the detecting coverage of the thermal image sensor, the body temperature monitoring system will capture a thermogram. Utilizing the software developed by CHINO [30], the captured thermogram can be read by BeagleBoard-xM. The system then reads the pixel of temperature and stores the thermogram as image files.

Third, the system accesses to the Arduino port through the universal asynchronous receiver/transmitter (UART) protocol to obtain the data of ambient temperature and relative humidity. The system uploads these sensed data to the database. As a result, various types of important information, including the time of the event, the body temperature of the passenger, and ambient temperature/relative humidity in the area, can be collected. Such information can be further analyzed if needed.

D. Back-end Relational Database

This study uses a back-end relational database (RDB) to store the sensed data. An RDB, widely used for data storage, is a digital database based on relational models [31]. It stores data using the mathematics concept of algebra of sets. RDBs use primary keys and foreign keys to establish a relation between each table and provide data indexes, which allow users to create, read, update, and delete data faster. Besides, database normalization is a necessary process in an RDB to reduce data redundancy and improve data integrity. Such a design simplifies the structure of RDBs to achieve the optimum structure. Accordingly, the RDB used in this study also follows the rules of normalization.

Fig. 3 shows a diagram of the RDB design. In the figure, there are six tables. Each table has a primary key, and some have a foreign key to connect with other. The six tables can provide two types of information: 1) device and 2) the information of each case. The device table records its own id and the device name. It connects to three tables, including place, building, and gate table through their foreign keys. These tables describe where the device is placed, and which building and gate the device is located at. After each device is settled, the system manager would record the device information in these tables. Then, each device will start to work and automatically transmit the collected data to a case table. This table includes the case id, device id, status id, body temperature, ambient temperature, and time of recording. Body temperature of person is measured by a thermal imaging sensor, and the ambient temperature is the measured by SHT 11 temperature sensor. The case table connects to a status table using the foreign key with the status id that indicates whether the case is normal or not.

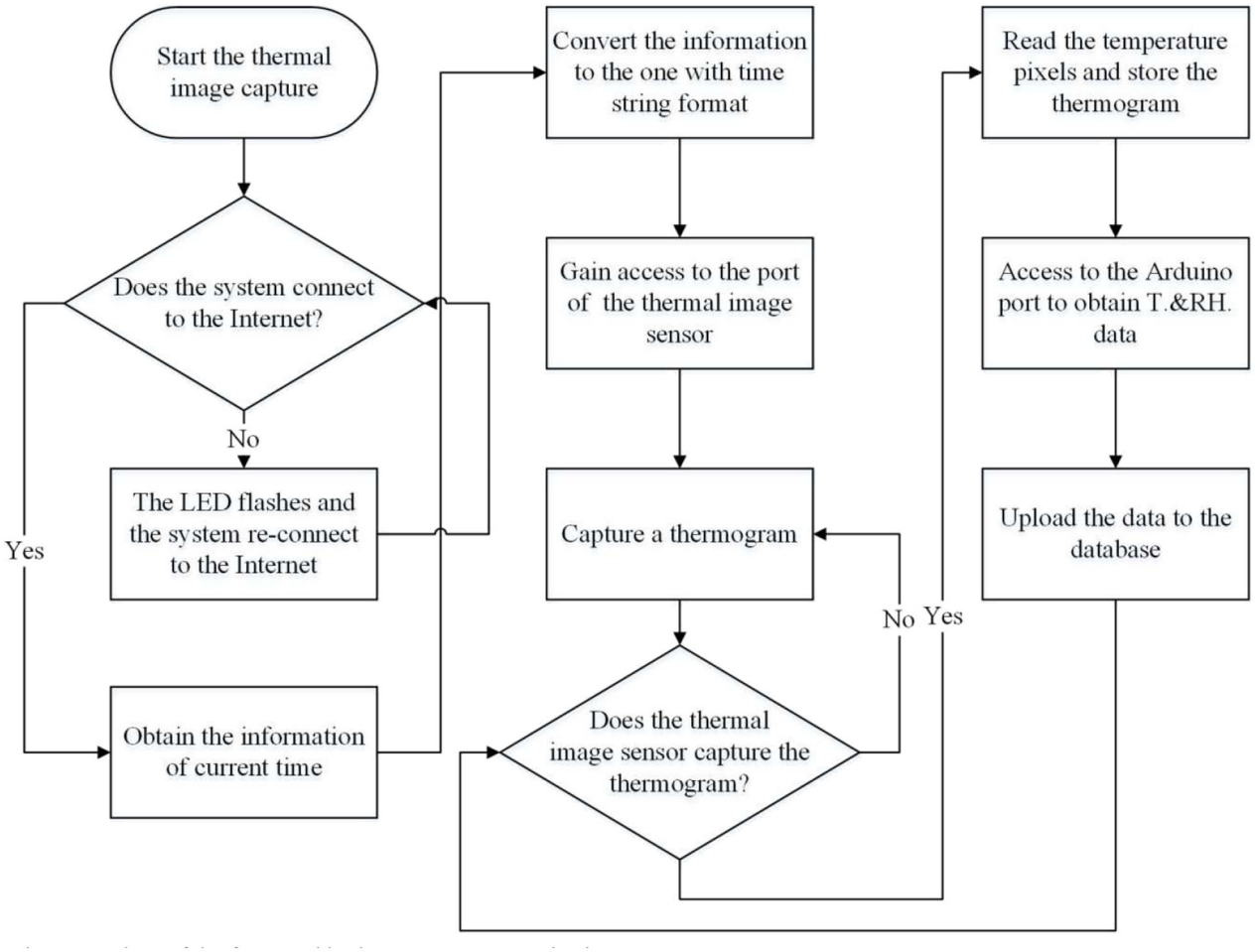

Fig. 2. Operation procedure of the front-end body temperature monitoring system.

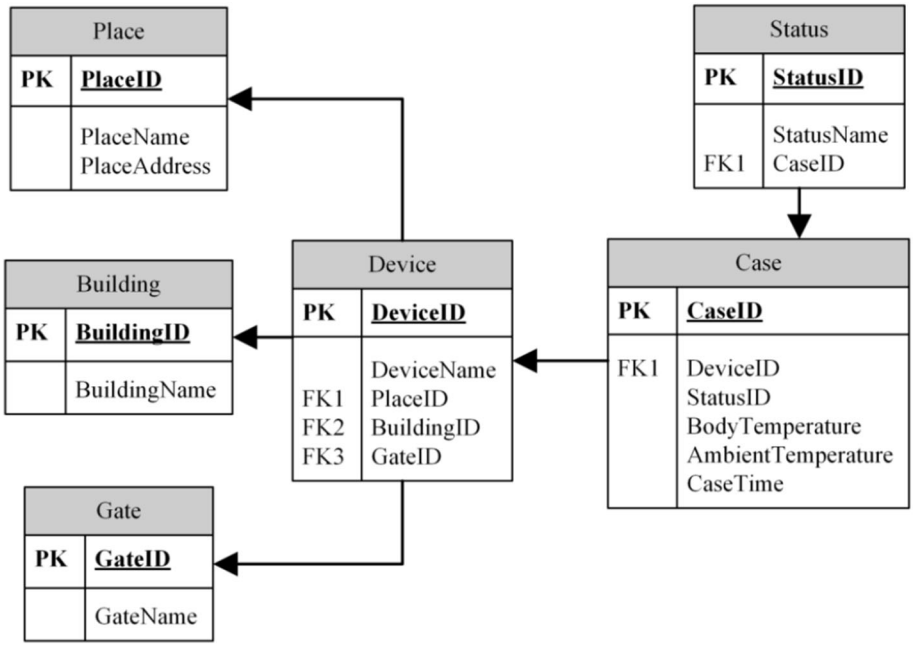

Fig. 3. Diagram of the RDB design.

E. Public Health Cloud Platform

In this study, a PHC platform is established to provide advanced services. The PHC platform is built with several rack servers. The collected data, such as thermal images, data of environmental temperature and relative humidity, and geographic information, are sent to the PHC platform via 03G

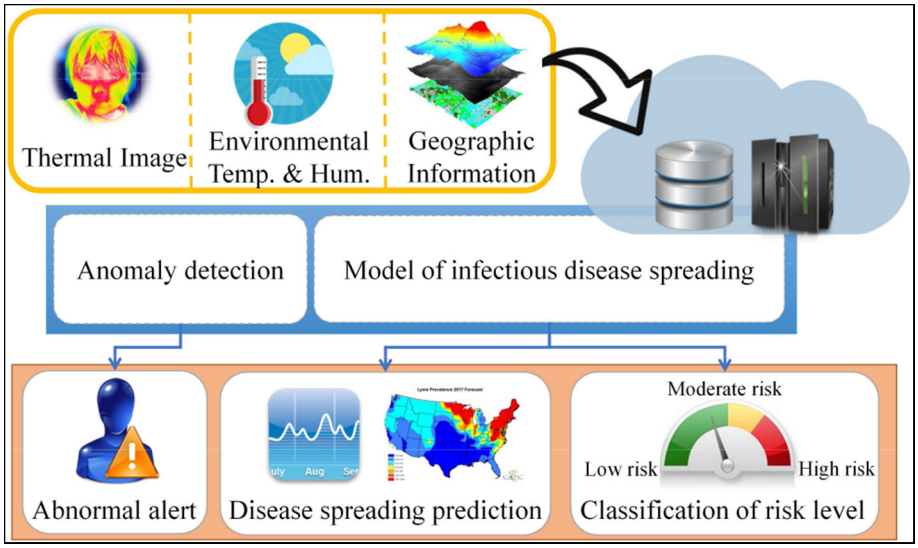

Fig. 4. Architecture of the PHC platform used in this study.

communication modules. The PHC platform is able to send out instant alerts if any anomalies occur, perform infectious disease spreading prediction, and provide classifications of risk levels. These services can help management or medical personnel to control infectious disease spreading. The architecture of the PHC platform is shown in Fig. 4, and each service is described as follows.

1) Instant Anomaly Alert: A short message service (SMS) message with the instant alert will be sent out to management and medical personnel when the body temperature monitoring system detects that a person's body temperature is higher than 37.5 °C, indicating that the person has a fever [32]. The record of all anomalies is stored in the database for further analysis. Such a service provides an important tool to fast control infectious disease spreading.

2) Classifications of Risk Levels and Infectious Disease Spreading Prediction: The record of each anomaly stored in the database also includes geographic information. Analyzing the historical data of the anomalies using a spatial correlation method [33], the trend of infectious disease spreading can be found. A four-state susceptible-latent-infective-removed (SLIR) mathematical model was built to simulate the progression of an epidemic and determine the exposure score for each classroom building [34]. In this study, the SLIR model was used to reflect the effect of space-time mobility to capture the frequency of contact among students in different classroom buildings. Therefore, the force of infection (λ) is defined as the rate at which susceptible individuals become infections [35], [36]. Since the indicator captures the intensity of the disease transmission, it is used as the score of the exposure to the infection risk in classroom building b at time-slice t as

$$\lambda_b(t) = \frac{\beta \times I_b(t)}{N_i} \tag{1}$$

where β is the transmission rate as a constant representing the transmissibility of a communicable disease, $I_b(t)$ and N_b are the infection number and the total population of classroom building b, respectively. Based on the records of mobility behavior of the person k, it can create the list of visited buildings $B_k = \{b_1, b_2, \ldots, b_n\}$, visited time $T_k = \{t_1, t_2, \ldots, t_n\}$, and visited duration (hours) $D_k = \{d_1, d_2, \ldots, d_n\}$. Then, we can determine the exposure in each building $R_k = \{\lambda_1, \lambda_2, \ldots, \lambda_n\}$ and the weight of the exposure by visited duration $R_k \times D_k/24$. The trajectories of mobility of an individual can be used to determine the person's exposure to the infection risk [34]. Therefore, the exposure score of the person k for the day (E_k) is expressed by the following as:

$$E_k = 1 - \prod_{b=1}^{n} \left(1 - R_k(b) \times \frac{D_k(b)}{24}\right). \tag{2}$$

According to the monitoring data provided by the body temperature monitoring system, five risk levels (extremely high, high, moderate, mild, and low) can be determined to an infected area through (1) and (2), and the risk levels are shown in Table II. Through this classification system, the public can easily get access to the risk information regarding the disease spreading. Based on mobility behavior of the users, the PHC platform could send the alert message via smart phone to the users, including individual exposure score and the risk level of the building when an epidemic breaks out. In the future, the risk level classification can be integrated into a decision support system.

On the other hand, the quantile regression method was first introduced to estimate the relationship between covariates and the quantile of response variable distribution in the economic research field [37]. The regression method is flexible, allowing covariates to exert various effects at distinct points of the distribution, and the estimation is robust to non-normality and skewed tails of the data distribution. In the recent years, this method has been used to analyze the spatial characteristics of DF incidences [38]. Therefore, the PHC platform in the proposed system utilizes the quantile regression method to investigate the underlying relationships between average daily fever incidences and potential risk factors to

TABLE II
RISK LEVEL CLASSIFICATION TABLE

Exposure score (E)	Risk level	Descriptions
$0.8 \le E < 1.0$	Extremely high	The disease is spread throughout the area.
$0.6 \le E < 0.8$	High	The disease is spread to the surrounding areas, and this area might be the next infected area.
$0.4 \le E < 0.6$	Moderate	This area might be the source of disease spreading; the risk for disease spreading is high in the area, but the risk is low in the surrounding areas.
$0.2 \le E < 0.4$	Mild	The risk of disease spreading is low in this area and the surrounding areas look normal.
$0 \le E < 0.2$	Low	The risk in this area and its surrounding areas are all low.

establish a prediction model of infectious disease spreading in the future.

IV. SYSTEM VERIFICATION AND DISCUSSION

Two tasks were performed to verify the proposed body temperature monitoring system: 1) body temperature and 2) environmental parameter sensing and sensed data transmission. The tests were conducted at the buildings of Department of Biomechatronics Engineering and Department of Geography in NTU.

A. System Verification Tests

As mentioned earlier, SHT11 was used in the body temperature monitoring system as a sensor to measure ambient temperature and relative humidity. To examine whether SHT11 can accurately measure temperature and relative humidity, a commercial electronic hygrometer (HT-3015, Lutron Electronic Enterprise Company, Ltd.) was employed and the temperature and relative humidity measured by HT-3015 were compared with those measured by SHT11. The sensing ranges of HT-3015 for the temperature and relative humidity are from 0 to 50 °C and from 0 to 95% RH, respectively, and the measurement resolution for temperature and relative humidity is 0.01 °C and 0.01% RH @ 23.5 °C, respectively. The measurement accuracy of HT-3015, i.e., (T, % RH), is (0.8 °C, 3.0 ∼ 4.0% RH). Other performance specifications of both SHT11 and HT-3015 are quite similar, except for the measuring ranges of the temperature.

To conduct a basic performance comparison between the sensors SHT11 and HT-3015, both sensors were placed at the top balcony of the Tomatake Hall at campus of NTU for long-term environmental data collection. The experimental site was a shaded area with good ventilation. During the experiment, the lowest and highest measured temperature were 27 °C and 35 °C, respectively. The measured relative humidity ranged from 45% to 85%.

A linear regression model was used to find the correlation between the temperatures measured by SHT11 and HT-3015, and the regression analysis results are shown in Fig. 5. It

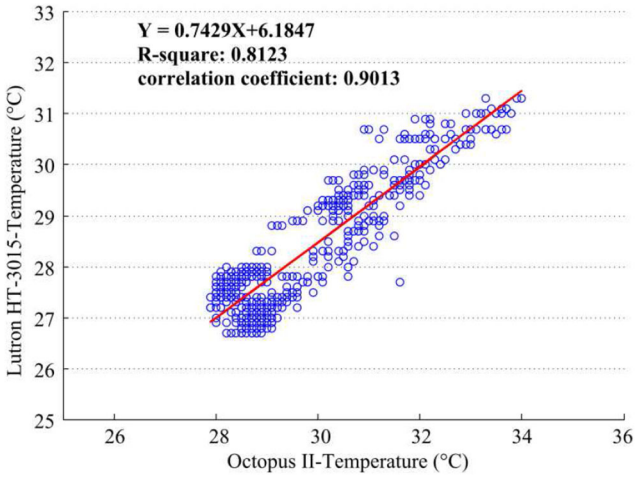

Fig. 5. Regression analysis results between the temperature data sets measured by SHT11 and HT-3015.

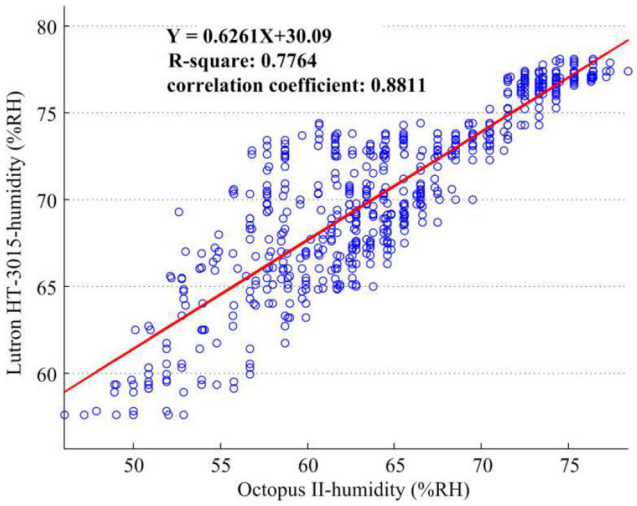

Fig. 6. Regression analysis results between the relative humidity readings measured by SHT11 and HT-3015.

is found that the correlation coefficient of the temperatures measured by the two sensors is 0.9013, and the coefficient of determination, R^2, is close to 0.8123. These results show a relatively small difference between the sensed data provided by the two sensors. Note that the HT-3015 (Lutron Electronic Enterprise Company, Ltd.) is a portable instrument that has been certified by ISO-9001, CE, IEC1010. Thus, the temperature readings provided by SHT11 are reliable and accurate.

The performance comparison between SHT11 and HT-3015 in measuring relative humidity was also conducted. Fig. 6 depicts the regression analysis results between relative humidity measurements by using SHT11 and HT-3015. The correlation coefficient between the relative humidity measured by both sensors is 0.8811. Such a result indicates that the differences between the relative humidity readings were slightly less than those of temperature readings, but SHT11 still provided satisfactory performance in measuring the relative humidity in an outdoor testing environment.

Furthermore, in the performance test of the thermal imaging sensor used by the proposed body temperature monitoring system, a thermal imaging sensor was placed on the top of the

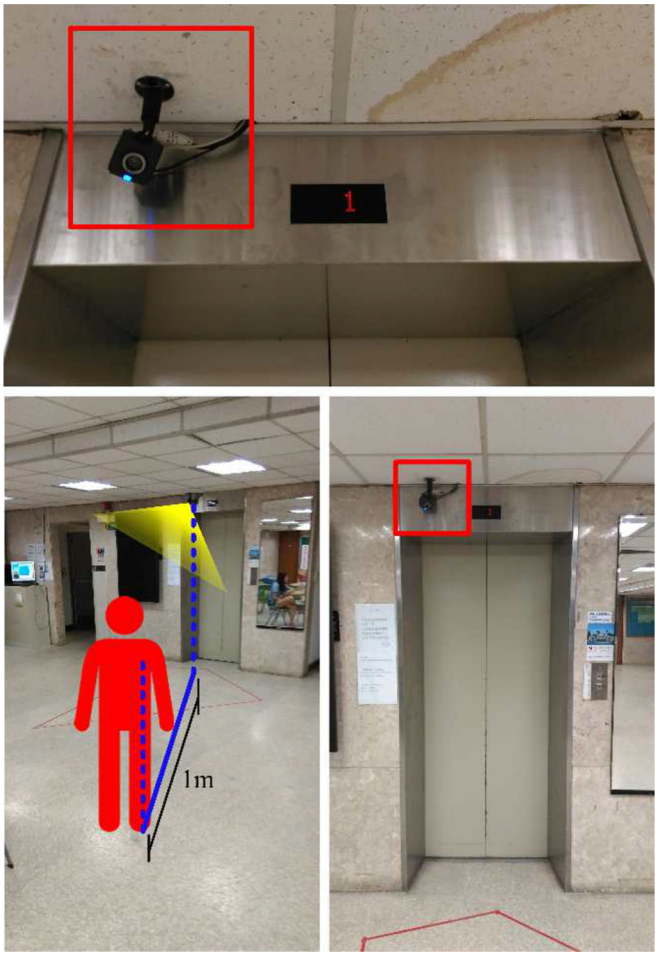

Fig. 7. Actual set-ups for the performance test of the thermal imaging sensor conducted at the buildings of Department of Geography in NTU.

elevator door at the buildings of Department of Geography in NTU and the detection shot was adjusted, so participants' body temperature image could be effectively captured. The actual set-ups of the test are shown in Fig. 7. The body temperatures of one hundred participants were first taken using an ear thermometer (IRT6500, Braun Company, Ltd.). Then the participants were asked to stay one meter away from the thermal imaging sensor for 11 s.

An infrared thermography first measures the infrared radiation emitted by an object, and then the energy detected is converted into a temperature value. However, since not all of the received radiation comes from the target object, to measure temperature accurately, the radiation from other sources (such as surrounding objects or the atmosphere) must be removed during the process of converting to a temperature value. This is called compensation. In this study, the total radiation received by the camera (W_{tot}) comes from three sources: 1) the emission of the target object (E_{obj}); 2) the emission of the surroundings; and 3) reflected by the object (E_{refl}), and the emission of the atmosphere (E_{atm}). It can be expressed as [39]

$$W_{\text{tot}} = E_{\text{obj}} + E_{\text{refl}} + E_{atm}. \tag{3}$$

In (3), the first source is the emission from the target object. A part of this reflected radiation is also absorbed by the atmosphere. The third component is the emission of the infrared radiation from the atmosphere. Further, it can be expressed as

$$E_{\text{obj}} = \varepsilon_{\text{obj}} \cdot \tau_{atm} \cdot \sigma \cdot \left(T_{\text{obj}}\right)^4 \tag{4}$$

$$E_{\text{refl}} = \left(1 - \varepsilon_{\text{obj}}\right) \cdot \tau_{atm} \cdot \sigma \cdot (T_{\text{refl}})^4 \tag{5}$$

$$E_{atm} = (1 - \tau_{atm}) \cdot \sigma \cdot (T_{atm})^4 \tag{6}$$

where ε_{obj} is the emissivity of the object, the σ is the Boltzmann constant, the t_{atm} is the transmittance of the atmosphere, T_{obj} is the temperature of the object, T_{refl} is the reflected temperature, and T_{atm} is the temperature of the atmosphere.

Substituting (4)–(6) in (3), we obtain that

$$W_{\text{tot}} = \varepsilon_{\text{obj}} \cdot \tau_{atm} \cdot \sigma \cdot \left(T_{\text{obj}}\right)^4 + \left(1 - \varepsilon_{\text{obj}}\right) \cdot \tau_{atm} \cdot \sigma \cdot (T_{\text{refl}})^4 + (1 - \tau_{atm}) \cdot \sigma \cdot (T_{atm})^4. \tag{7}$$

Therefore, the temperature of the object can be calculated as

$$T_{\text{obj}} = \sqrt[4]{\frac{W_{\text{tot}} - \left(1 - \varepsilon_{\text{obj}}\right) \cdot \tau_{atm} \cdot \sigma \cdot (T_{\text{refl}})^4 - (1 - \tau_{atm}) \cdot \sigma \cdot (T_{atm})^4}{\varepsilon_{\text{obj}} \cdot \tau_{atm} \cdot \sigma}}. \tag{8}$$

To solve (8), the following parameters must be supplied: the emissivity of the object (ε_{obj}), the reflected temperature (T_{refl}), the transmittance of the atmosphere (t_{atm}), and the temperature of the atmosphere (T_{atm}). The transmittance of the atmosphere is generally estimated using the distance from the object to the camera and the relative humidity. In general, this value is very close to one. The temperature of the atmosphere is obtained using a common thermometer. However, the emittance of the atmosphere is very close to zero ($1 - t_{atm}$), so this parameter has little influence on the temperature measurement. On the other hand, the emissivity of the object and the reflected skin temperature in the clinical practice is known [39]. Therefore, the body temperature can be estimated by the infrared thermograms. A uniform thermogram is output based on the infrared radiation input. The image size is 60 × 60 pixels, and the thermal sensitivity is less than 50 mK (0.05 °C). An example of the thermogram stored in the database is shown in Fig. 8. The maximum temperature on the head of each participant, i.e., body temperature, is captured [39], and body temperature data are further transmitted to the database every 2 s. The rate of the export compliant frame of the sensor is around 9 Hz, can be accessed sequentially via the serial peripheral interface protocol. Using the thermal imaging camera, the temperature differences can be visualized, and the temperature information can be obtained immediately while maintaining a sufficient safe distance from those who may have been infected.

Then, the mean absolute percentage error (MAPE) and the root mean square error (RMSE) were used as the indexes to examine the differences between the body temperature measured by the ear thermometer and the body temperature detected by the thermal imaging sensor. The MAPE was selected because it is presented as percentage, which is easy to be understood and would not be influenced by the magnitude of the data. The MAPE of using the thermal imaging sensor

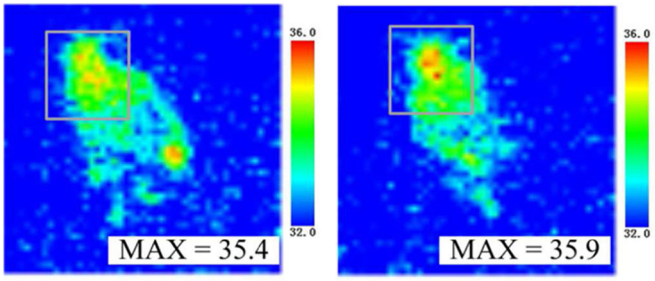

Fig. 8. Body temperature captured by the thermal imaging sensor.

to measure body temperature is defined as

$$\text{MAPE} = \frac{\sum \left| \frac{\text{Actual\_temp} - \text{Thermal\_temp}}{\text{Actual\_temp}} \right|}{\text{Test}_{\text{total}}} \times 100\% \quad (9)$$

where the $\text{Test}_{\text{total}}$ is the total number of tests in the whole experiment.

On the other hand, the RMSE was adopted to examine the sensing accuracy of the thermal imaging sensor, because it emphasizes the large deviations between the values, so it is sensitive to outliers. The RMSE of using thermal imaging sensor is defined as

$$\text{RMSE} = \sqrt{\frac{\sum(\text{Actual\_temp} - \text{Thermal\_temp})^2}{\text{Test}_{\text{total}}}}. \quad (10)$$

The detailed comparison results are shown in Table III. The ear thermometer and thermal imaging sensor each measured a total of 100 body temperatures. The mean of body temperatures was 36.724 °C and 35.942 °C for the ear thermometer and thermal imaging sensor, while the standard deviation was 0.357 °C and 0.386 °C, respectively. The temperatures measured by the ear thermometer were from 36.000 °C to 37.300 °C, and they were slightly higher than those measured by the thermal imaging sensor. The MAPE was 2.15%, and the RMSE was 1.004 °C.

B. Relationships Between the Environmental Temperature and the Measured Body Temperature

To have a better understanding of what caused the temperature difference, we further designed an experiment to find out the relationships between the environmental temperature and the measured body temperature. The set-ups of the experiment are shown in Fig. 9. The experiment was set up at the meeting room of the Department of Biomechatronics Engineering in NTU. The thermal imaging sensor was attached to a cabinet 1.7 m above the ground. The environmental temperature was controlled at 27 °C, 24 °C, and 21 °C by an air conditioner after it operated for 30 min to reach a stable temperature. There were 30 participants in the experiment, and their body temperature was both measured by an ear thermometer and a thermal imaging sensor. Each participant was asked to stay in front of a gray line and the distance between the corner of the cabinet and the gray line was about 0.75 m.

Then, the body temperature measured by the ear thermometer (T_{body}), the temperature detected by the thermal imaging sensor (T_{img}), and the environmental temperature measured by a Celsius thermometer (T_{env}) in the experiment were further analyzed. Fig. 10 shows the distribution of the temperatures obtained from the three environmental temperatures. It can be seen that T_{img} is scattered on the right side of the figure when the environment temperature is close to 27 °C. But when the environment temperature is at 24 °C and 21 °C, the measured body temperatures did not have an obvious pattern but concentrate on the middle part and left side of the figure.

To further examine the relationship between the environmental temperature and the body temperature measured by the two sensors, two variables were introduced in this study. Δ_1 was defined as $T_{\text{img}} - T_{\text{env}}$ and Δ_2 was defined as $T_{\text{body}} - T_{\text{env}}$. Fig. 11 shows the distributions of T_{body} and Δ_1. It is found that Δ_1 falls between 7.5 °C and 8.8 °C and T_{body} falls between 35.0 °C and 37.0 °C, when the environment temperature is close to 27 °C. When the environment temperature is at24 °C, by contrast, Δ_1 falls between 9.1 °C and 10.6 °C, and T_{body} falls between 35.0 °C and 36.7 °C. When the environment temperature is at 21 °C, Δ_1 falls between 11.2 °C and 13.1 °C, and T_{body} falls between 34.4 °C and 36.8 °C.

Moreover, a liner regression analysis that involved two variables, T_{env} and the mean value of Δ_1, was conducted. The results are shown in Fig. 12, and the equation of the regression line is shown as

$$\Delta_{1,\text{avg}} = -0.65T_{\text{env}} + 25.6. \quad (11)$$

The coefficient of determination, R^2, for the regression line is rather high, indicating T_{env} and the mean value of Δ_1 are highly correlated. Using (11), the mean value of Δ_1 can be expressed by T_{env}.

Another linear regression analysis that involved T_{env} and the mean value of Δ_2 was also conducted. The results are shown in Fig. 13, and the equation of the regression line is given by

$$\Delta_{2,\text{avg}} = -0.367T_{\text{env}} + 10.867. \quad (12)$$

The coefficient of determination, R^2, for the regression line is also high, indicating T_{env} and the mean value of Δ_2 are also highly correlated. Hence, the mean value of Δ_2 can be presented by T_{env} using (12).

Now, the effect of ambient temperature on the body temperature measured by the thermal imaging sensor can be further eliminated by using a liner regression method. The body temperature regression line can be derived from combining the (11) and (12), given as below

$$T_{\text{body}} = T_{\text{env}} + \Delta_1 + \Delta_2 + 0.1. \quad (13)$$

This equation can be utilized in real scenarios. If T_{env} and T_{img} are known, T_{body}(regression) can be calculated using (13). The Δ_1 falls between 8.05 °C and 11.95 °C, and Δ_2 falls between 0.9661 °C and 3.1663 °C when the environmental temperature between 21 °C and 27 °C, respectively. Then, the MAPE and RMSE for T_{body}(regression) and T_{body}(real) at 21 °C, 24 °C, and 27 °C are calculated, and the results are shown in Table IV. The MAPE is equal to 0.06%, 0.05%, and 0.01%, when the environmental temperature remains at 21 °C, 24 °C, and 27 °C, respectively. The RMSE is equal to 0.0236 °C, 0.0216 °C, and 0.0161 °C when the environmental temperature remains at 21 °C, 24 °C, and 27 °C, respectively.

TABLE III
BODY TEMPERATURES MEASURED BY THE EAR THERMOMETER AND THERMAL IMAGING SENSOR

Measurement type	Body temperature (°C)				Evaluation index	
	Mean (°C)	Std.	Min.	Max.	MAPE (%)	RMSE (°C)
Ear thermometer	36.724	0.357	36.000	37.300	2.15%	1.004
Thermal imaging sensor	35.943	0.386	34.600	36.800		

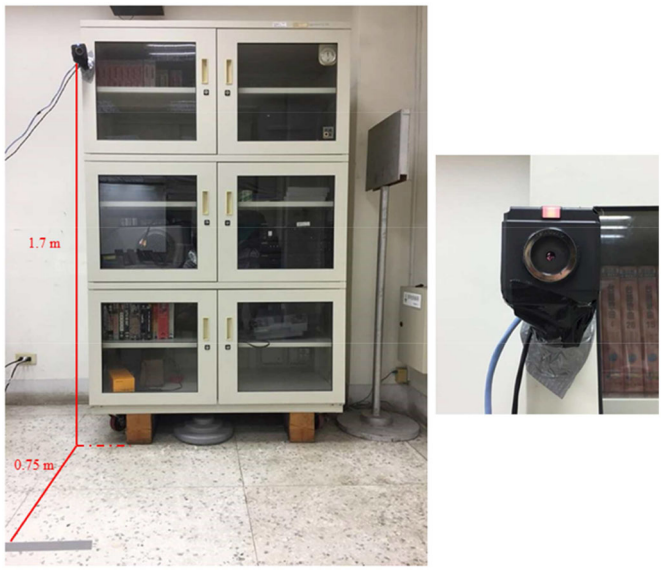

Fig. 9. Experimental set-ups for the environmental temperature and the body temperature measured by a thermal imaging sensor conducted at the meeting room of the Department of biomechatronics Engineering in NTU.

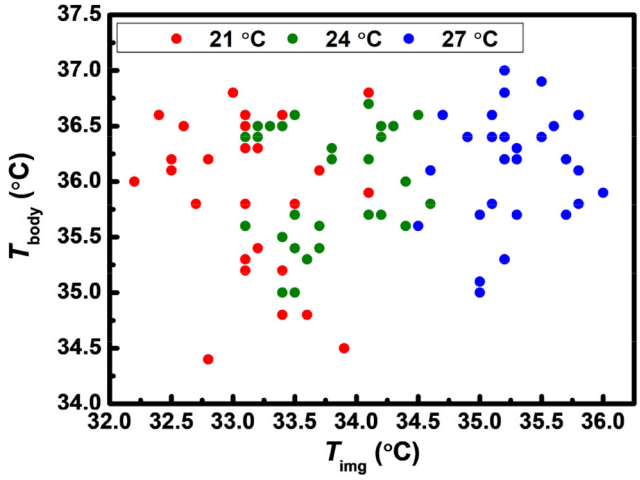

Fig. 10. Distribution of T_{body} and T_{img}.

Based on the results, the difference between the T_{img} and T_{body} is 0.782 °C, which means that the estimation of the true body temperature is affected by environmental temperatures. The body temperature measured by the thermal imaging sensor can still accurately represent the actual body temperature after doing calibrations that take environmental temperatures into account. All of the mentioned calibrations were also integrated into this proposed system. First, the front-end body temperature monitoring system can monitor the body temperature with thermography inspection method and measured the

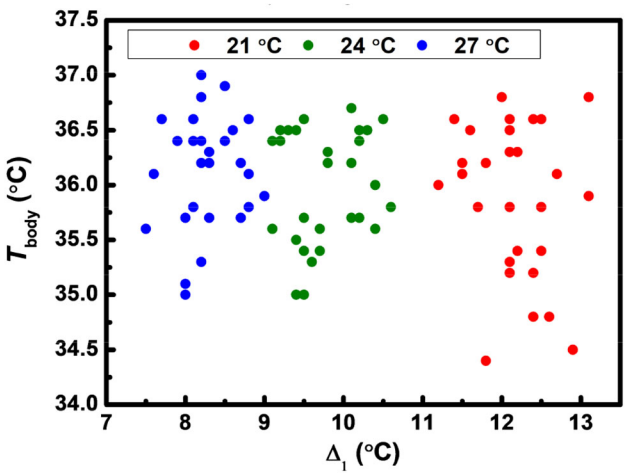

Fig. 11. Distribution of T_{body} and Δ_1.

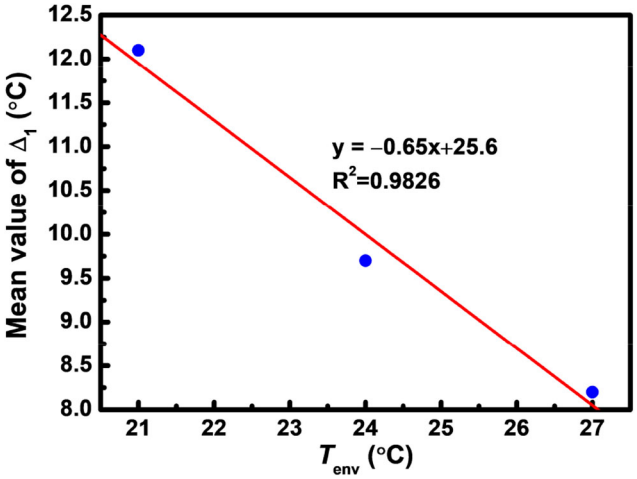

Fig. 12. Regression analysis results for T_{env} and the mean value of Δ_1.

ambient temperature/relative humidity with IoT architecture. Through analyzing the sensing data, the PHC platform can provide the important disease outbreak information, such as the instant alert for any anomalies, infectious disease spreading prediction, and risk level classification. Further, it can be used to improve the management and control of the infectious disease spreading.

C. *Efficiency of Using Thermal Imaging Sensor*

An experiment was conducted to examine the efficiency of using a thermal imaging sensor to measure body temperature. The time required to measure body temperature using different sensing devices was compared. Five people participated in the experiment. They entered a room and their temperatures were taken using an ear thermometer and a thermal imaging sensor.

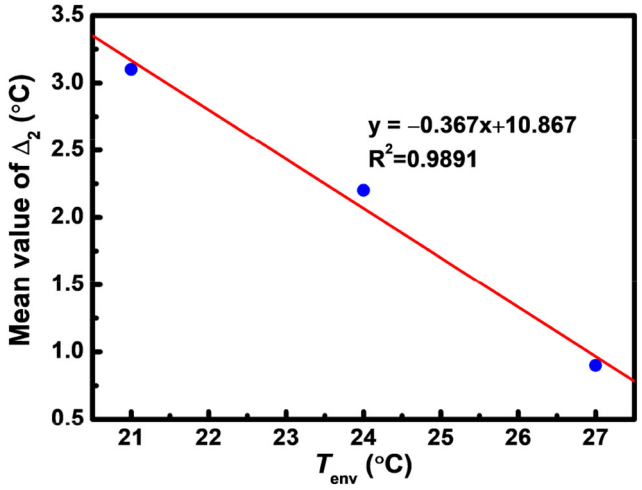

Fig. 13. Regression analysis results for T_{env} and the mean value of Δ_2.

The experiment procedure was repeated five times for each participant. The time spent on measuring body temperature was recorded.

The experimental results are shown in Table V. Compared to using an ear thermometer, utilizing a thermal imaging sensor reduces the time spent on measurement of body temperature by 60.8% in average. The benefit of using thermal imaging sensors to measure body temperature would become much greater when a large number of people are waiting for taking their temperature. These experimental results indicate that using the proposed body temperature monitoring system would largely reduce the time required for measuring body temperature.

V. Case Study: System Implementation at National Taiwan University

In this study, the campus of NTU was selected for system implementation and verification. The population density of universities is high, so students and faculty members at universities are at high risk of getting infected by flu and other infectious diseases. Especially for universities, where students go to classes held in different rooms, and they meet many students at different class. An infectious disease would be fast spread if one student got infected. Thus, a university campus is a great place to test the proposed body temperature monitoring system. The radius resolution of the thermal image sensor used in the study is 60×60 pixels, and the captured thermographic images, therefore, are not able to show naked bodies. These images are solely used in determining body temperature. Thus, personal privacy of the detected passengers is not likely to be violated.

Further, a number of the body temperature monitoring systems with thermal imaging sensors could be installed at the gates of different buildings, including a department building, a classroom building, and a library. To verify the proposed system, a RDB was established to store the monitoring data, a user interface was developed for back-end platform, and an alert system that provided the SMS was used to send out infectious disease outbreak information. The implementation of these three elements is described as follows.

A. Implementation of the Relational Database

The RDB was built by PHP 5.2.1 and MySQL 5.0.27, which is an open-source RDB, to provide database management service with phpMyAdmin 2.9.2.

B. Graphical User Interface

Fig. 1 has depicted that the PHC of the proposed monitoring system can provide the services of infectious disease spreading prediction, risk level classification, instant anomaly alert, etc. To do these services, a visualized and intuitive graphical user interface (GUI) was created. The GUI can provide the users a convenient way to inquire the status of the services provided by the system, e.g., the statistical data of collected body temperature cases and anomaly cases, and indicating risk level of the targeted buildings. Users could browse the monitoring data shown on the GUI via an online website. On the website, all of the monitoring data were laid out on a campus map. By doing so, the spreading of infectious diseases could be clearly seen. Fig. 14 shows a GUI example, where the daily monitoring data, locations of targeted buildings, risk levels are shown. In this case, the thermal imaging sensors are installed at three buildings: 1) Tomatake Hall (Position 1); 2) Main Library (Position 2); and 3) multipurpose classroom building (Position 3). The numbers of the anomalies and the total monitored cases are also shown on the interface, as indicated in the lowest row in Fig. 14. In addition, a light indicator was designed to warn users. The indicator was green under a normal condition, and it would change to red if the number of the daily anomalies reaches five. There were 64, 176, and 158 people monitored at Position 1, 2, and 3, respectively. Five anomalous cases were found at Tomatake Hall (Position 1). System users would receive an alter message that contained the related information, such as time, position, and the number of anomalous cases. The campus could be further partitioned into a number of zones with different risk levels, and the spatial clustering of the high-risk areas would be identified. Class suspension could be considered for buildings located in the high-risk areas.

The information provided by the GUI can help administration personnel at universities follow the guidelines for epidemic disease control. The risk levels can be evaluated through individual exposure scores and the monitoring data provided by the proposed system. Then, the public is able to receive the risk information regarding the disease spreading. For example, Table VI shows the guidelines for responding to epidemic diseases at NTU. The responses to epidemic diseases are classified into four levels, from no infected cases found at the campus to infected cases reported at the campus. According to the table, an active temperature monitoring system should be adopted at level 3. As mentioned earlier, traditional body temperature monitoring methods cost too much to run continuously. The interruption of active body temperature monitoring may miss many infected cases. The proposed body temperature system can substitute for traditional body temperature monitoring methods, so that the university can fast control any infected cases. Another important contribution of the proposed

TABLE IV
RMSE AND MAPE FOR T_{body}(REGRESSION) AND T_{body}(REAL)

T_{env} (°C)	Δ_1 (°C)	Δ_2 (°C)	T_{body}(regression) (°C)	T_{body}(real) (°C)	MAPE	RMSE (°C)
21	11.95	3.1663	36.2163	36.2	0.06%	0.0236
24	10	2.0662	36.1662	36.2	0.05%	0.0216
27	8.05	0.9661	36.1161	36.1	0.01%	0.0161

TABLE V
TIME REQUIRED FOR AN EAR THERMOMETER AND A THERMAL IMAGE TO MEASURE BODY TEMPERATURE

Participant Number	Average required time using an ear thermometer (sec.)	Average required time using a thermal imaging sensor (sec.)	Time saving percentage (%)
No.1	2.73	1.00	63.20
No.2	2.50	1.11	55.48
No.3	2.74	1.02	62.50
No.4	2.58	1.02	60.51
No.5	2.77	1.05	62.29

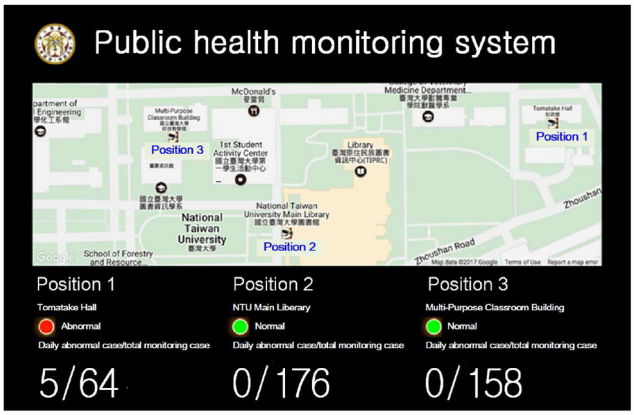

Fig. 14. Monitoring information provided by the GUI designed for NTU infectious disease control.

monitoring system is that the monitoring data are updated and shown on a graphic user interface in real time.

C. SMS Alert Mechanism

An SMS alert mechanism was established for users who pay attention to the infectious disease control at the campus. Using their cellphones, users subscribe the notification service, so the PHC of the proposed monitoring system will inform the users if any anomalies occur. If the monitoring system finds any anomalies, an alert would be sent to users. The alert message in SMS format sent by the system is shown in Fig. 15. With the proposed monitoring system, people who have a fever can be quickly found, and the spreading of infectious diseases can be fast controlled. Based on the alert message, it would be safer if an individual visits classroom buildings with lower disease spreading risks while avoiding buildings with high risks. The proposed monitoring system will play a key role in epidemic prevention.

D. System Comparison

The great pioneer in thermometry of the human body was Carl Reinhold August Wunderlich. Among his several significant publications was his treatise on "Temperature in

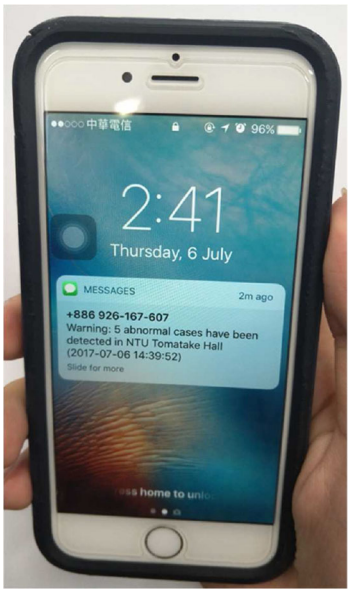

Fig. 15. Alert message sent by the proposed monitoring system.

Diseases, a manual of medical thermometry" in 1868. He set out numerous statements of clinical significance especially relating to fever, the course of temperature related to increases and decreases of fever, and the importance of regular and consistent measurement to provide objective evidence of the status of the patient [40]. The axillary measurements were used which gave only an estimate of peripheral temperature and the measurements were performed in a nonstandardized way [41]. The infrared ear thermometer (IRET) is an alternative to other noninvasive methods to measure body temperature. As the probe of the IRET is placed approximately 1.5 cm away from the tympanic membrane, the reading is a mix of heat from the tympanic membrane and the aural canal [42]. Noteworthy is that the other noninvasive sites, such as the rectal, oral, and axillary, show limitations in measurement accuracy owing to placement of the thermometer [43]. On the other hand, the needs for body temperature measurement and using the thermal image as a noninvasive means of determining skin temperature were always present [44].

TABLE VI
GUIDELINES FOR RESPONSES TO EPIDEMIC DISEASES AT NTU

Level	Epidemic situation	Responses
Level 1	No case found at the campus	1. promoting self-health management 2. maintaining a clean environment
Level 2	Cases reported in the campus, but no case found at the campus	1. taking one's temperature 2. sterilizing hands in the public area 3. avoiding a large-scale event
Level 3	Cases found at the campus	1. placing infected cases in quarantine 2. starting active temperature monitoring
Level 4	Cases found at the campus, causing more infected cases	1. partial or whole school suspension 2. banning large-scale events

However, the above-mentioned studies just measured the body temperature by the contact or noninvasive methods. They didn't store the personal body temperature and not analyze the risk level of the local building. In this proposed system, it comprised of the front-end body temperature monitoring system, a back-end RDB, and the PHC platform. The body temperature of a person can be monitored with thermography inspection with IoT architecture and used to analyze the score of exposure to the risk. The proposed system can also provide the important disease outbreak information, such as the instant alert for any anomalies and risk level classification. Through this proposed system, the management and control of the infectious disease spreading can be improved effectively.

VI. CONCLUSION

This study proposed a high-accuracy body temperature monitoring system and PHC platform based on the IoT architecture, and this system was successfully implemented in campus buildings. In this system, a thermal imaging sensor was adopted to collect thermograms, while a temperature/relative humidity sensor was used to collect environmental temperature and relative humidity data. All monitoring data were integrated by the BeagleBoard-xM module and transmitted to a cloud for further analysis via a 3G communication module. A number of experiments were conducted to examine the performance of the proposed monitoring system, including system verification and efficiency improvement. These results show that the proposed system is stable and can accurately measure environmental temperature/relative humidity and body temperature. Moreover, the body temperature measured by the thermal imaging sensor can be calibrated based on the regression analysis results that take environmental temperature into consideration. Other experimental results show that the efficiency of using thermal imaging sensors is high. After including the environmental temperature in the calibrations, the mean MAPE and RMSE of the body temperature is 0.04% and 0.0204 °C, respectively. Compared to using ear thermometers, thermal imaging sensors could reduce the time spent on measuring body temperature by 60.8% in average. Using thermal imaging sensors, therefore, is able to fast acquire accurate body temperature data.

Note that there are still some limitations of this work. First of all, missed detections (MDs), which refer to failing to detect people with a high fever, may occur. This issue greatly relates to the selection of proper parameters for the liner regression method of body temperature measurements. In this study, we did not conduct the body temperature measurements for the patients with a fever, so it is impossible to evaluate MD cases. Based on the current results of this study, the proposed system can be only used to find a reasonable body temperature sensing range for normal people in different environmental situations. Therefore, the other limitation of the proposed system is that false alarms (FAs) might be also possible sends out to users. To reduce the opportunities of MDs and FAs, for suspicious cases (e.g., coughing and having a chronically runny nose for no apparent reason), their body temperature would be manually measured again. Besides, it is found that environmental variations may affect the detection accuracy, causing more MDs and FAs. This study has tested the effect of environmental temperatures, one of the main sources of environmental variations, on body temperature measurements. Based on the test results, the difference between the T_{img} and T_{body} is 0.782 °C, which suggests that environmental temperatures indeed affect the estimation of the true body temperature. The impacts brought by other environmental variations (such as the distance between the detected object and the camera) on the detection accuracy, however, will be tested in future studies. In addition, the risk level classification proposed by this study can be integrated with an expert decision system in the future to provide real-time prediction of the spreading of infectious diseases, and help management or medical personnel control infectious disease spreading.

ACKNOWLEDGMENT

The authors would like to thank the members of their research team for their valuable suggestions and contributions to this work.

REFERENCES

[1] M. N. K. Boulos *et al.*, "Crowdsourcing, citizen sensing and sensor Web technologies for public and environmental health surveillance and crisis management: Trends, OGC standards and application examples," *Int. J. Health Geograph*, vol. 10, p. 67, Dec. 2011.

[2] (2009). *Pandemic (H1N1)*. Accessed: Jan. 22, 2016. [Online]. Available: http://www.who.int/csr/don/2010_01_22/en

[3] *Middle East Respiratory Syndrome Coronavirus (MERS-CoV)*. Accessed: Sep. 27, 2017. [Online]. Available: http://www.who.int/emergencies/mers-cov/en/

[4] *SARS (Severe Acute Respiratory Syndrome)*, Centers Dis. Control, R.O.C., Taipei, Taiwan. Accessed: Nov. 24, 2016. [Online]. Available: https://www.cdc.gov.tw/english/info.aspx?treeid=E&nowtreeid=E&tid=9E

[5] *Dengue Fever*, Centers Dis. Control, R.O.C., Taipei, Taiwan. Accessed: Nov. 24, 2016. [Online]. Available: https://www.cdc.gov.tw/english/info.aspx?treeid=E&nowtreeid= E&tid=D76AD76D26365478

[6] Y. K. Axelrod and M. N. Diringer, "Temperature management in acute neurologic disorders," *Neurol. Clin.*, vol. 26, no. 2, pp. 585–603, May 2008.

[7] K. B. Laupland, "Fever in the critically ill medical patient," *Crit. Care Med.*, vol. 37, no. 7, pp. S273–S278, Jul. 2009.

[8] E. F. Ring, H. McEvoy, A. Jung, J. Zuber, and G. Machin, "New standards for devices used for the measurement of human body temperature," *J. Med. Eng. Technol.*, vol. 34, no. 4, pp. 249–253, May 2010.

[9] K. Ashton, "That 'Internet of Things' thing," *RFID J.*, vol. 22, no. 7, pp. 97–114, 2009.

[10] E. Y. K. Ng, G. J. L. Kawb, and W. M. Chang, "Analysis of IR thermal imager for mass blind fever screening," *Microvasc. Res.*, vol. 68, no. 2, pp. 104–109, Sep. 2004.

[11] D. M. Bell, "Public health interventions and SARS spread, 2003," *Emerg. Infect. Dis.*, vol. 10, no. 11, pp. 1900–1906, Nov. 2004.

[12] R. K. St John, A. King, D. de Jong, M. Bodie-Collins, S. G. Squires, and T. W. Tam, "Border screening for SARS," *Emerg. Infect. Dis.*, vol. 11, no. 1, pp. 6–10, Jan. 2005.

[13] P. Gope and T. Hwang, "BSN-Care: A secure IoT-based modern healthcare system using body sensor network," *IEEE Sensors J.*, vol. 16, no. 5, pp. 1368–1376, Mar. 2016.

[14] S. M. Riazul Islam, D. Kwak, M. D. Humaun Kabir, M. Hossain, and K.-S. Kwak, "The Internet of Things for health care: A comprehensive survey," *IEEE Access*, vol. 3, pp. 678–708, 2015.

[15] L. Catarinucci *et al.*, "An IoT-aware architecture for smart healthcare systems," *IEEE Internet Things J.*, vol. 2, no. 6, pp. 515–526, Dec. 2015.

[16] C. Pereira, A. Pinto, D. Ferreira, and A. Aguiar, "Experimental characterization of mobile IoT application latency," *IEEE Internet Things J.*, vol. 4, no. 4, pp. 1082–1094, Aug. 2017.

[17] N. Hema Rajini, "A comprehensive survey on Internet of Things based healthcare services and its applications," in *Proc. 3rd Int. Conf. Comput. Methodol. Commun. (ICCMC)*, Erode, India, Mar. 2019, pp. 483–488.

[18] S. Vicini, S. Bellini, A. Rosi, and A. Sanna, "An Internet of Things enabled interactive totem for children in a living lab setting," in *Proc. 18th Int. ICE Conf. Eng. Technol. Innovat.*, Munich, Germany, 2012, pp. 1–10.

[19] M. Vazquez-Briseno, C. Navarro-Cota, J. I. Nieto-Hipolito, E. Jimenez-Garcia, and J. D. Sanchez-Lopez, "A proposal for using the Internet of Things concept to increase children's health awareness," in *Proc. 22nd IEEE Int. Conf. Elect. Commun. Comput. (CONIELECOMP)*, Cholula, Mexico, 2012, pp. 168–172.

[20] N. Nigar and M. N. Uddin, "A mHealth platform using transfer learning and Internet of Things to improve children's health consciousness and behavior," in *Proc. 21st Int. Conf. Comput. Inf. Technol. (ICCIT)*, Dhaka, Bangladesh, 2018, pp. 1–5.

[21] A. J. Jara, F. J. Belchi, A. F. Alcolea, F. Santa, M. A. Zamora-Izquierdo, and A. F. Gómez-Skarmeta, "A pharmaceutical intelligent information system to detect allergies and adverse drugs reactions based on Internet of Things," in *Proc. 8th IEEE Int. Conf. Pervasive Comput. Commun. Workshops (PERCOM Workshops)*, Mannheim, Germany, 2010, pp. 809–812.

[22] G. Yang *et al.*, "A health-IoT platform based on the integration of intelligent packaging, unobtrusive bio-sensor, and intelligent medicine box," *IEEE Trans. Ind. Informat.*, vol. 10, no. 4, pp. 2180–2191, Nov. 2014.

[23] V. Koutkias, V. Kilintzis, N. Beredimas, and N. Maglaveras, "Leveraging medication safety through mobile computing: Decision support and guidance services for adverse drug event prevention," in *Proc. EAI 4th Int. Conf. Wireless Mobile Commun. Healthcare Transf. Healthcare Through Innovat. Mobile Wireless Technol. (MOBIHEALTH)*, Athens, Greece, Nov. 2014, pp. 19–22.

[24] A. B. H. Altaweel, L. Abusalah, and D. M. Qato, "Near field communication detection system for drug-drug interactions," *Procedia Comput. Sci.*, vol. 140, pp. 314–323, Nov. 2018.

[25] A. Dohr, R. Modre-Opsrian, M. Drobics, D. Hayn, and G. Schreier, "The Internet of Things for ambient assisted living," in *Proc. IEEE 7th Int. Conf. Inf. Technol. New Gener. (ITNG)*, Las Vegas, NV, USA, 2010, pp. 804–809.

[26] M. Haghi *et al.*, "A flexible and pervasive IoT-based healthcare platform for physiological and environmental parameters monitoring," *IEEE Internet Things J.*, vol. 7, no. 6, pp. 5628–5647, Jun. 2020.

[27] Z. Pang, J. Tian, and Q. Chen, "Intelligent packaging and intelligent medicine box for medication management towards the Internet-of-Things," in *Proc. Int. Conf. Adv. Commun. Technol. (ICACT)*, Pyeongchang, South Korea, 2014, pp. 352–360.

[28] I. Laranjo, J. Macedo, and A. Santos, "Internet of Things for medication control: E-health architecture and service implementation," *Int. J. Rel. Qual. E-Healthcare*, vol. 2, no. 3, pp. 1–15, Jul.–Sep. 2013.

[29] A. Mirea and A. Albu, "Automated system for medication stocks management," in *Proc. 22nd Int. Conf. Syst. Theory Control Comput. (ICSTCC)*, Sinaia, Romania, 2018, pp. 529–534.

[30] *CHINO TP Series Thermal Imaging Sensor*. Accessed: Nov. 10, 2016. [Online]. Available: http://www.chino.co.jp/english/download/pdf/PSE-708.pdf

[31] W. Kent, "A simple guide to five normal forms in relational database theory," *Commun. ACM*, vol. 26, no. 2, pp. 120–125, Feb. 1983.

[32] W. T. Chiu *et al.*, "Infrared thermography to mass-screen suspected SARS patients with fever," *Asia–Pac. J. Public Health*, vol. 17, no. 1, pp. 26–28, 2005.

[33] D. Wartenberg, "Multivariate spatial correlation: A method for exploratory geographical analysis," *Geogr. Anal.*, vol. 17, no. 4, pp. 263–283, Oct. 1985.

[34] T. H. Wen, C. S. Hsu, C. H. Sun and J. A. Jiang, "A location-based client-server framework for assessing personal exposure to the transmission risks of contagious diseases," in *Human Dynamics Research in Smart and Connected Communities* (Human Dynamics in Smart Cities), S. L. Shaw and D. Sui, Eds. Cham, Switzerland: Springer, Feb. 2018, pp. 133–148.

[35] D. Balcan, B. Gonçalves, H. Hu, J. J. Ramasco, V. Colizza, and A. Vespignani, "Modeling the spatial spread of infectious diseases: The global epidemic and mobility computational model," *J. Comput. Sci.*, vol. 1, no. 3, pp. 132–145, Aug. 2010.

[36] L. Sattenspiel, *The Geographic Spread of Infectious Diseases*. Princeton, NJ, USA: Princeton Univ. Press, 2009.

[37] R. Koenker and G. Bassett Jr., "Regression quantiles," *Econometrica*, vol. 46, no. 1, pp. 33–50, Jan. 1978.

[38] H.-C. Chiu, H. Hannemann, K. J. Heesom, D. A. Matthews, and A. D. Davidson, "High-throughput quantitative proteomic analysis of dengue virus type 2 infected A549 cells," *PLoS ONE*, vol. 9, no. 3, Mar 2014, Art. no. e93305.

[39] R. Usamentiaga, P. Venegas, J. Guerediaga, L. Vega, J. Molleda, and F. G. Bulnes, "Infrared thermography for temperature measurement and non-destructive testing," *Sensors*, vol. 14, pp. 12305–12348, Jul. 2014.

[40] C. A. Wunderlich, *On the Temperature in Diseases, A Manual of Medical Thermometry*. London, U.K.: New Sydenham Soc., 1871.

[41] P. A. Mackowiak, "Clinical thermometric measurements," in *Fever Basic Mechanisms and Management*, 2nd ed., P. A. Mackowiak, Ed. Philadelphia, PA, USA: Lippincott Raven, 1997, pp. 27–33.

[42] J. Y. Lefrant *et al.*, "Temperature measurement in intensive care patients: Comparison of urinary bladder, oesophageal, rectal, axillary, and inguinal methods versus pulmonary artery core method," *Intensive Care Med.*, vol. 29, no. 3, pp. 414–418, 2003.

[43] "Assessment of fever," in *Physiology, Immunology, Measurement in Clinical Practice*, E. Grodzinsky and M. Sund Levander, Eds. Malmö, Sweden: Gleerups, 2015.

[44] F. J. Ring, "Pioneering progress in infrared imaging in medicine," *Quant. InfraRed Thermogr. J.*, vol. 11, no. 1, pp. 57–65, 2014.

Joe-Air Jiang (Senior Member, IEEE) received the M.S. and Ph.D. degrees in electrical engineering from National Taiwan University (NTU), Taipei, Taiwan, in 1990 and 1999, respectively.

He is currently a Distinguished Professor of Biomechatronics Engineering with NTU. He was also the Chairman of Taiwan Institute of Biological Mechatronics, NTU from 2016 to 2019. He published 422 papers in different journals and conference proceedings, was granted 65 intellectual patents from USA and Taiwan, and edited one book with Springer-Verlag. He is currently the principal investigator of many large-scale integration projects funded by the Ministry of Science and Technology and the Council of Agriculture of the Executive Yuan, Taiwan. He and his research team got interviewed by the BBC and Discovery channel, and his research achievements have been broadcasted around the world via BBC and Discovery Channel in 2013 and 2014, respectively. His specialties in power transmission system are computer relaying, solar generation system, fault detection, fault classification, fault location, power quality event analysis, and smart grid system. Besides, his areas of interests are diverse, which cover wireless sensor network /Internet of Things technologies, automatic system for agro-ecological monitoring with WSN/IoT, bio-mechatronics, smart grid, solar generation systems, power system, computer relaying, bio-effects of electromagnetic wave, and low-level laser therapy.

Dr. Jiang received research awards and best paper awards at various occasions. He was awarded by the 38th Ten Outstanding Agriculturist from Taiwan District of Kiwanis International in 2014 and the Academic Achievement Award from Chinese Institute of Agricultural Machinery in 2010, respectively. He received the Outstanding Research Award and the Outstanding Technology Transfer Contribution Award from the Ministry of Science and Technology in 2020, the Outstanding Research Innovation Award from NTU in 2020, the Award of Outstanding Electrical Engineering Professor from Chinese Institute of Engineers in 2016, respectively, the Lifetime Achievement Award for International Outstanding Inventors from the seventh International Innovation and Invention Competition in 2016, the Award of Continuing Dedicated Service and Research Contribution from Intel-NTU Connected Context Computing Center in 2015, the Award of Intel Labs Distinguished Collaborator from Intel in 2016, the Excellence in Teaching Awards from National Taiwan University in 2004, 2012, 2013, 2016, and 2019, the Excellence in Teaching Awards from College of Bioresources and Agriculture at NTU in 2014, 2015, 2017, and 2020, and an Excellent Mentor Award from NTU in 2011. His achievements on innovation and international collaboration also earned him awards. The great contributions to the higher education continuously have been done by him since 2001 so that he received the Excellent Teacher Award from the Ministry of Education, Taiwan, in 2018. He is an Active Researcher.

Jen-Cheng Wang received the B.S. degree in electronic engineering from Chang Gung University, Taoyuan, Taiwan, in 2005, and the Ph.D. degree in bio-industrial mechatronics engineering from the National Taiwan University (NTU), Taipei, Taiwan, in 2013.

From 2013 to 2016, he was a Senior Engineer and the Research and Development Engineer with the Epitaxy Engineering Department, EPISTAR Corporation, Hsinchu, Taiwan. Since 2016, he has been a Postdoctoral Researcher with the Department of Electrical Engineering, Department of Biomechatronics Engineering, and the Education and Research Center for Bio-Industrial Automation, NTU, where he is currently a Postdoctoral Researcher with the Department of Biomechatronics Engineering. He has published 54 papers in different international journals and 110 papers of conference proceedings, was granted three intellectual patents from USA. and Taiwan, and was wrote one chapter of book in Springer-Verlag. He led research efforts on the IoT-based smart grids, industrial automation, remote sensing services, and data mining. His current research interests include the data mining and analysis, machine learning and deep learning, smart grid, wireless sensor networks, optoelectrical characterization of photovoltaic module, III–V compound semiconductor materials and optoelectrical devices, and novel low-dimensional photonic nanomaterials and nanodevices.

Chao-Liang Hsieh received the B.S. degree in mechatronics engineering from the National Changhua University of Education, Changhua, Taiwan, in 2016, and the M.S. degree in bio-industrial mechatronics engineering from the National Taiwan University, Taipei, Taiwan, in 2018.

His research interests are in the areas of machine learning, smart city, and wireless sensor network.

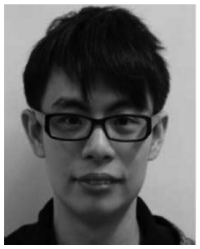

Kai-Sheng Tseng born in Kaohsiung, Taiwan, in 1993. He received the B.S. degree with the National Taiwan Ocean University, Keelung, Taiwan, in 2015, and the M.S. degree in bio-industrial mechatronics engineering with the National Taiwan University, Taipei, Taiwan, in 2019.

His research interests are in the areas of automatic control, computer science, wireless sensor network, and smart grid.

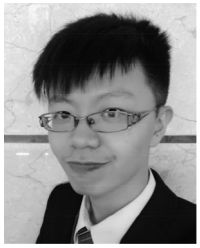

Zheng-Wei Ye born in Taipei, Taiwan, in 1992. He received the Bachelor of Science and master's degrees in bio-industrial mechatronics engineering from the National Taiwan University, Taipei, Taiwan, 2014 and 2017, respectively.

His research of interests includes data analysis, machine learning, and deep learning.

Lin-Kuei Su born in Taoyuan, Taiwan, in 1992. He received the B.S. degree in electrical engineering from the National Chung Hsing University, Taichung, Taiwan, in 2014, and the M.S. degree in bio-industrial mechatronics engineering from the National Taiwan University, Taipei, Taiwan, in 2016.

His research interests are in the areas of data analysis, smart grid, and wireless sensor network.

Chih-Hong Sun received the Ph.D. degree in geography from the University of Georgia, Athens, GA, USA, in 1986.

He is a Professor with Geography Department, National Taiwan University (NTU), Taipei, Taiwan, where he served as a Chairman of the Geography Department from August 1994 till July 1997. He served as the Director of the Global Change Research Center, NTU from 1998 to 2004 and the Executive Secretary of the Commission on Sustainable Development Research, National Science Council, Washington, DC, USA, from March 1998 to June 2000. His research specialties are in geographic information system, spatial decision support system, hazards mitigation, and sustainable development. His recent researches are concentrated in developing intelligent spatial decision support system for natural hazards mitigation and for sustainable development issues.

Tzai-Hung Wen was born in Taipei, Taiwan, in 1974. He received the Ph.D. degree in bioenvironmental systems engineering from the National Taiwan University, Taipei, Taiwan, in 2006.

He was a Postdoctoral Fellow of Academia Sinica from 2006 to 2007. His early independent research and teaching experiences started in 2008, as being a Project Assistant Professor with the Institute of Epidemiology, NTU, where he has been the Faculty Member of the Department of Geography. His research topics focus on modeling geospatial and temporal process in human environment.

Dr. Wen received the Wu Da-Yu Memorial Award from the Ministry of Science and Technology in 2015, which is the most prestigious recognition for young investigators in Taiwan.

Jehn-Yih Juang received the Ph.D. degree from the Nicholas School of the Environment and Earth Sciences, Duke University, Durham, NC, USA, in 2007.

He is currently an Associate Professor with the Department of Geography, National Taiwan University, Taipei, Taiwan. The focus of his research field is to quantify and characterize the process of the interaction between the land surface and the atmosphere from micro to regional scales. The first topic is to quantify the fluxes passing through the interface of the terrestrial biosphere and the near surface atmospheric boundary-layer, and characterize how these ecosystem responses interact with the environment over different temporal and spatial scales. The other research field is to explore how the changes in land use and land cover alter the microenvironment, especially the energy budgets, and air quality and the hydrological cycle in the micro- to regional-scale environment.